

Potential phase control of chromium oxide thin films prepared by laser-initiated organometallic chemical vapor deposition

Ruihua Cheng, C. N. Borca, and P. A. Dowben^{a)}

Department of Physics and Astronomy and the Center for Materials Research and Analysis (CMRA), Behlen Laboratory of Physics, University of Nebraska–Lincoln, Lincoln, Nebraska 68588-0111

Shane Stadler and Y. U. Idzerda

Naval Research Laboratory, Materials Physics Branch, Washington, D.C. 20375

(Received 31 July 2000; accepted for publication 28 November 2000)

We have used laser-initiated chemical vapor deposition to grow the chromium oxide thin films through the oxidation of $\text{Cr}(\text{CO})_6$ in an oxygen environment. While both Cr_2O_3 and CrO_2 are present in the film, the relative weight of each phase depends on the oxygen partial pressure. The Curie temperature of the film increases and approaches the bulk T_C of CrO_2 (397 K) as the partial oxygen pressure is increased. © 2001 American Institute of Physics. [DOI: 10.1063/1.1343846]

The high electron polarization, in addition to the half-metallic character of the surface¹ makes CrO_2 an attractive material for spin-tunnel junctions² (where very large tunneling magnetoresistance is expected), as well as other magnetoresistive devices.^{3,4} The insulating antiferromagnetic chromium oxide Cr_2O_3 has a Néel temperature 307 K and is suitable for tunnel junction barriers⁴ both below and above the Néel temperature. The ferromagnetic chromium oxide CrO_2 with T_C 397 K (Ref. 5) has been predicted to be half metallic (metallic for one spin direction while insulating for the other spin direction) by band structure calculations,^{1,6–9} though Kulatov and Mazin found CrO_2 to be insulating in both spin directions.¹⁰ Evidence of 80% to 100% polarization, consistent with the half-metallic character of CrO_2 , were observed in spin-polarized photoemission,¹¹ vacuum tunneling,¹² and Andreev scattering.^{13,14} Biquadratic coupling and/or giant magnetoresistance, observed above the Néel temperature for Fe/Cr multilayers,^{15,16} may be enhanced in $\text{CrO}_2/\text{Cr}_2\text{O}_3$ multilayers because of the lower Néel temperature and insulating character of Cr_2O_3 . Below the Néel temperature, unidirectional magnetic anisotropy and exchange bias at the interface between the ferromagnetic and antiferromagnet layers may be expected, as in the case of NiFe/NiO,^{17,18} NiFe/FeMn,¹⁹ and Fe/Cr (Ref. 20) bilayer and multilayer systems.

It is difficult to fabricate CrO_2 ultrathin films using conventional methods because CrO_2 is metastable. This is not altogether bad, as the two phases $\text{CrO}_2/\text{Cr}_2\text{O}_3$ system exhibits higher magnetoresistance than the pure material.⁴ The oxidation of the organometallic complex hexacarbonyl $\text{Cr}(\text{CO})_6$ has the potential for selective deposition of CrO_2 .^{21–23} These studies have established that chromium oxides are the thermodynamic sink of chromium hexacarbonyl decomposition²³ and the oxidation is further aided by the presence of an ambient oxygen background.^{21,22} By modifying this organometallic chemical vapor deposition procedure, we have been able to fabricate the ferromagnetic and antiferromagnetic chromium oxides. Here, we describe both the growth and the magnetic properties of these films.

The growth of the chromium oxide films were carried out on Si(111) substrates in an ultrahigh vacuum chamber, maintained at a base pressure at 1.0^{-9} Torr or less. This chamber was designed for laser initiated chemical vapor deposition as described elsewhere.^{24,25} The photolytic decomposition and oxidation of $\text{Cr}(\text{CO})_6$ was performed by a commercial nitrogen laser with the main emission line at 337 nm (corresponding to 3.69 eV). The ambient oxygen (O_2) atmosphere was varied from 1×10^{-7} to 1×10^{-5} Torr relative to the $\text{Cr}(\text{CO})_6$ partial pressure of 1×10^{-5} Torr, uncorrected for ionization gauge cross section and monitored with a quadruple mass spectrometer operated in pulse counting mode.

The x-ray adsorption spectroscopy (XAS) and magnetic circular dichroism (MCD) spectra were taken at the U4B beam line at the National Synchrotron Light Source at Brookhaven National Laboratory. The photon beam was set $\sim 75\%$ helicity and the incident beam was 45° off from the surface normal. For magnetizing the sample, a 200 Oe pulsed field was applied in plane. The MCD spectra were recorded by alternating the magnetization at every photon energy with a fixed helicity of the incident light.

The nonmagnetic chromium oxide phase is dominated by Cr_2O_3 crystallites with a pronounced preferential orientation. Figure 1 shows the light polarization dependent Cr L edge [Fig. 1(a)] and O K edge [Fig. 1(b)] XAS of the chromium oxide film fabricated with an ambient of 5×10^{-7} Torr oxygen partial pressure. At energies above the Cr L_3 edge, the spectra are dominated by two peaks, around 577.7 eV and 579 eV, followed by another two peaks above the L_2 edge, around 586.9 eV and 588.5 eV. The oxygen spectra [Fig. 1(b)] are first dominated by a large feature between 532 and 535 eV. This oxygen XAS spectra is similar to the expected XAS spectra of Cr_2O_3 (Ref. 26) while the chromium L edge spectra are consistent with a mixed oxide.¹ There is a strong dependence of the spectra on the light incidence angle, particularly at the oxygen edge. This originates from the orientation of $\text{O}-2p-\text{Cr}-3d$ hybrid states with respect to the crystalline axes.²⁶

The polarization dependence of the XAS and the x-ray diffraction (XRD) results indicate texture growth in our films. The XRD pattern, shown as the inset in Fig. 1, indi-

^{a)}Author to whom correspondence should be addressed; electronic mail: pdowben@unl.edu

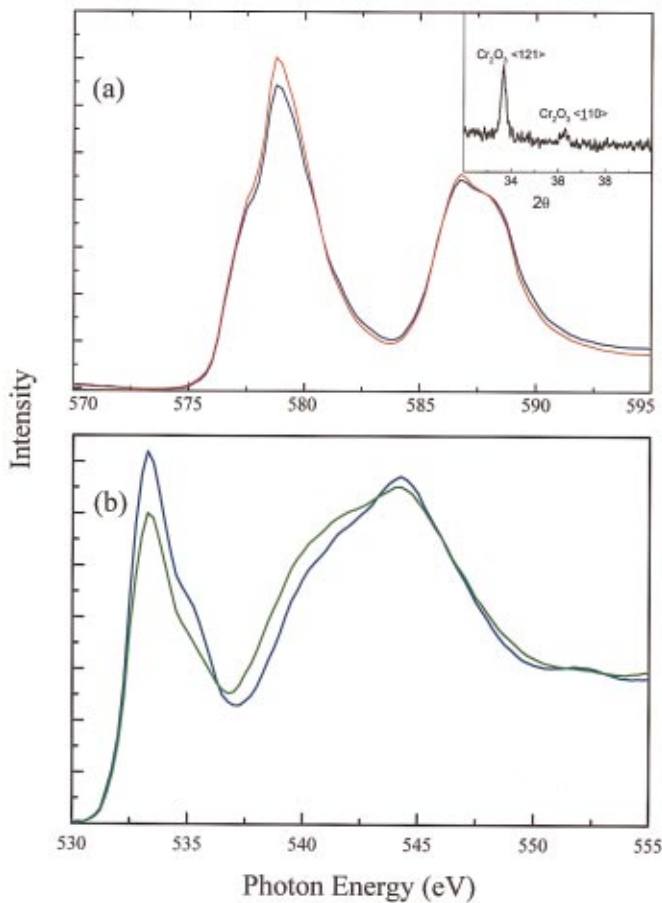


FIG. 1. (Color) XAS polarization dependence. The polarization dependent XAS for Cr L edge of film fabricated in an ambient O_2 (5×10^{-7} Torr) background is shown in (a). The data shown as red line was taken at a 70° incident angle, while the blue solid line shows the XAS data for normal incidence (pure s -polarized light). The polarization dependence of XAS at O K edge is shown in (b). The data shown as blue is for normal light incidence (pure s polarized), and green is for a 55° light incidence angle. The XRD data for the film fabricated with ambient O_2 pressure 5×10^{-6} Torr relative to the $Cr(CO)_6$ partial pressure of 1×10^{-5} Torr is shown as the inset.

cates that the Cr_2O_3 rich samples grown on Si(111) adopt a rhombohedral structure ($R\bar{3}C$ space group). Strong texture growth is characteristic of other chromium oxide thin films grown by chemical vapor deposition.^{2,14} As we increase the

partial O_2 pressure, the fraction of Cr_2O_3 decreases. We find no evidence of the Cr_2O_5 or CrO_3 phases in XRD but do not exclude the possibility of a very small minority fraction. In the case of CrO_2 rich samples, the structure identification in XRD is not conclusive due to the fact that both Si(111) and tetragonal $CrO_2(110)$ diffraction peaks overlap.

The coexistence of CrO_2 and Cr_2O_3 is evident in the hysteresis loop obtained at 100 K, with the applied magnetic field in the plane of the film, shown in Fig. 2(a). The curve shown is for the sample fabricated with an O_2 pressure of 2×10^{-7} Torr relative to the $Cr(CO)_6$ partial pressure of 1×10^{-5} Torr. The coercive force for left-hand side half loop is 250 Oe while for right-hand side half loop it is 150 Oe. The fact that the coercive field is often not symmetric in our films suggests uniaxial magnetic anisotropy,¹⁷⁻²⁰ or exchange coupled bias^{27,28} between the textured domains of antiferromagnetic Cr_2O_3 and CrO_2 . In addition, antiferromagnetic hysteresis is observed at higher fields [Fig. 2(a)]. Figure 2(b) is Cr L edge MCD signal of film fabricated with ambient O_2 5×10^{-6} Torr. Note the evidence for magnetic order in the CrO_2 t_{2g} and e_g bands for both L_2 and L_3 edges.²⁹ The signal indicates the strong ferromagnetic character of CrO_2 ,²⁶ though we attribute some e_g like weight to small amount of Cr_2O_3 , even for samples fabricated at these higher oxygen partial pressures.

Figure 3 shows the magnetization versus temperature obtained from superconducting quantum interference device magnetometry. The critical temperature clearly depends upon the oxygen partial pressure at the time of film fabrication. Samples fabricated at 2×10^{-7} Torr oxygen partial pressure relative to the $Cr(CO)_6$ partial pressure of 1×10^{-5} Torr exhibit the Curie temperature of 345 ± 10 K. Samples fabricated at the higher 1×10^{-6} Torr oxygen partial pressure (relative to the $Cr(CO)_6$ partial pressure of 1×10^{-5} Torr) exhibit the higher Curie temperature of about 390 ± 10 K. The absence of a sharp T_c and the presence of a long tail in the magnetization curves (Fig. 3), near the critical temperature, are again suggestive of a two phase system. When we increase the O_2 partial pressure, the amount of CrO_2 phase increases and the critical temperature approaches the expected T_c of CrO_2 .⁴ The samples characterized by Au-

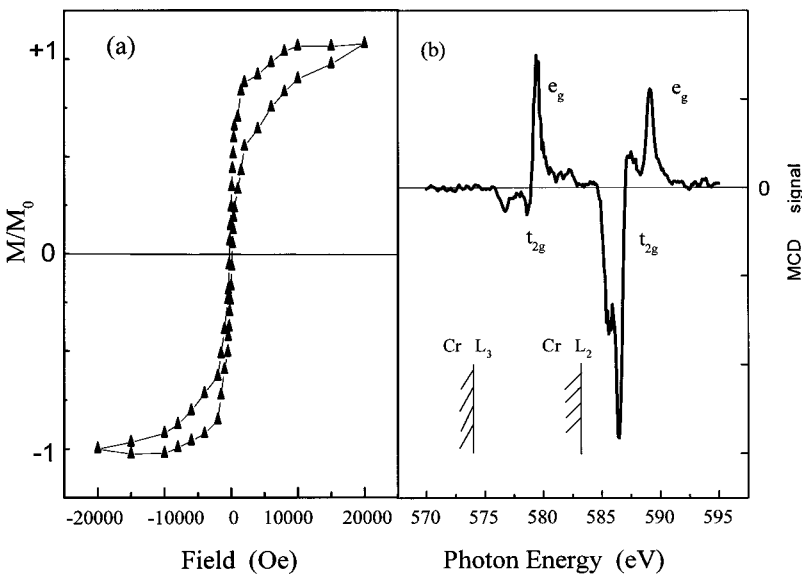


FIG. 2. (a) Hysteresis loop was taken at 100 K of the film with ambient O_2 pressure 2×10^{-7} Torr. (b) The Cr $L_{2,3}$ edge MCD signal was taken at room temperature of the film fabricated with ambient O_2 pressure 5×10^{-6} Torr relative to the $Cr(CO)_6$ partial pressure of 1×10^{-5} Torr.

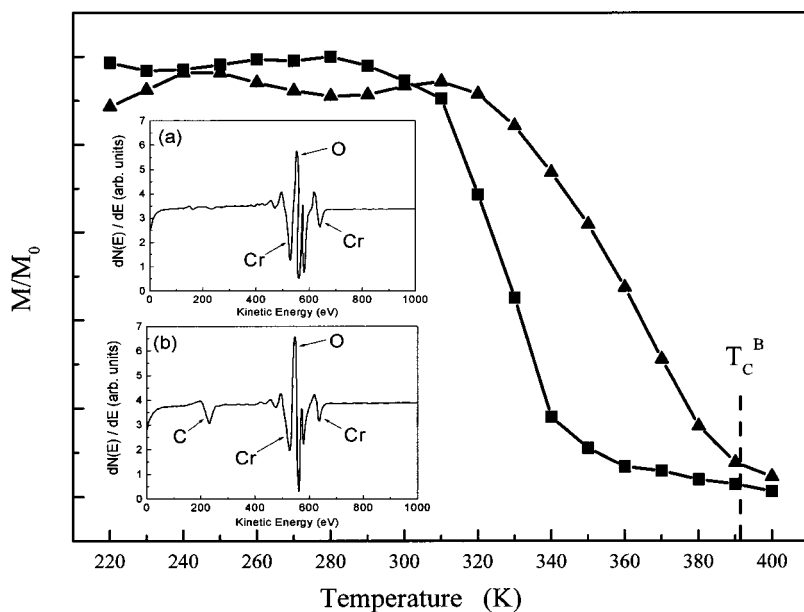


FIG. 3. The magnetization (M) vs temperature (T) at an applied field of $H=500$ Oe. Data are shown for two films: the data (■) were taken from the film fabricated in an O_2 pressure of 2×10^{-7} Torr relative to the $Cr(CO)_6$ partial pressure of 1×10^{-5} Torr, while the data (▲) were taken from the film fabricated in an O_2 pressure of 1×10^{-6} Torr relative to the $Cr(CO)_6$ partial pressure of 1×10^{-5} Torr. AES of the photolytic oxidative chemical vapor deposition of Cr_2O_3 and CrO_2 (for high and low O_2 partial pressure, respectively) are shown as insets (a) and (b), respectively.

ger electron spectroscopy (AES), as shown in the insets, Fig. 3(a) presents the Auger spectrum characteristic to a Cr_2O_3 rich sample, and Fig. 3(b) is representation for a CrO_2 rich sample. The spectra show clearly that the Cr signal increases relative to the overlapping oxygen signal for the Cr_2O_3 samples as compared to the CrO_2 samples.

In summary, we have used laser-initiated chemical vapor deposition and oxidation of $Cr(CO)_6$ to make chromium oxide thin films. Like the photolysis of chomyl chloride (CrO_2Cl_2),^{14,30} the advantage of this technique is selective area deposition and strong texture growth in the films. Phase control of this system, at the surface or boundary layers, appears to be far more likely than the potential half metallic systems $La_{0.65}Sr_{0.35}MnO_3$ (Ref. 31) and $NiMnSb$ (Ref. 32) where surface segregation readily occurs. The MCD results provide indications of magnetic ordering in the unoccupied t_{2g} and e_g bands of L_2 and L_3 chromium edges while the magnetization measurements show that the relative weight of both Cr_2O_3 and CrO_2 phases depends on and can be controlled by the oxygen partial pressure. The T_C of the film increases and approaches the bulk T_C of CrO_2 (397 K) as we increase the partial oxygen pressure.

This work was supported by NSF through Grant No. DMR-98-02126, the Center for Materials Research and Analysis (CMRA) and the Nebraska Research Initiative at the University of Nebraska.

¹H. van Lueken and R. A. de Groot, Phys. Rev. B **51**, 7176 (1995).

²A. M. Bratkovsky, Phys. Rev. B **56**, 2344 (1997).

³S. S. Manoharan, D. Elefant, G. Reiss, and J. B. Goodenough, Appl. Phys. Lett. **72**, 984 (1998); X. W. Li, A. Gupta, T. R. McGuire, P. R. Duncombe, and Gang Xiao, J. Appl. Phys. **85**, 5585 (1999); K. Suzuki and P. M. Tedrow, Phys. Rev. B **58**, 11597 (1998).

⁴J. D. M. Coey, A. E. Berkowitz, L. L. Balcells, F. F. Putris, and A. Barry, Phys. Rev. Lett. **80**, 3815 (1998).

⁵J. S. Kouvel and D. S. Rodbell, J. Appl. Phys. **38**, 979 (1967).

⁶K. Schwarz, J. Phys. F: Met. Phys. **16**, L211 (1986).

⁷S. Matar, G. Demazeau, J. Sticht, V. Eyert, and J. Kübler, J. Phys. I **2**, 315 (1992).

⁸M. A. Korotin, V. I. Anisimov, D. I. Khomskii, and G. A. Sawatzky, Phys. Rev. Lett. **80**, 4305 (1998).

⁹S. P. Lewis, P. B. Allen, and T. Sasaki, Phys. Rev. B **55**, 10 253 (1997).

¹⁰E. Kulatov and I. I. Mazin, J. Phys.: Condens. Matter **2**, 343 (1990).

¹¹K. P. Kämper, W. Schmitt, G. Güntherodt, R. J. Gambino, and R. Ruf, Phys. Rev. Lett. **59**, 2788 (1987).

¹²R. Weisendanger, H.-J. Güntherodt, G. Güntherodt, R. J. Gambino, and R. Ruf, Phys. Rev. Lett. **65**, 247 (1990).

¹³R. J. Soulen, J. M. Byers, B. Nadgorny, T. Ambrose, S. F. Cheng, P. R. Broussard, C. T. Tanaka, J. Nowak, J. S. Moodera, A. Barry, and J. M. D. Coey, Science **282**, 85 (1998); R. J. Soulen, M. S. Osofsky, B. Nadgorny, T. Ambrose, P. Broussard, and S. F. Cheng, J. Appl. Phys. **85**, 4589 (1999).

¹⁴W. J. DeSisto, P. R. Broussard, T. F. Ambrose, B. E. Nadgorny, and M. S. Osofsky, Appl. Phys. Lett. **76**, 3789 (2000).

¹⁵E. E. Fullerton, K. T. Riggs, C. H. Sowers, S. D. Bader, and A. Berger, Phys. Rev. Lett. **75**, 330 (1995).

¹⁶S. Adenwalla, G. P. Felcher, E. E. Fullerton, and S. D. Bader, Phys. Rev. B **53**, 2474 (1996).

¹⁷W. H. Meiklenjohn and C. P. Bean, Phys. Rev. **102**, 1413 (1956); A. P. Malozemoff, Phys. Rev. B **37**, 7673 (1988); A. P. Malozemoff, Phys. Rev. B **35**, 3679 (1985); N. C. Koon, Phys. Rev. Lett. **78**, 4865 (1997).

¹⁸G. Ju, L. Chen, A. V. Nurmikko, R. F. C. Farrow, R. F. Marks, M. J. Carey, and B. A. Gurney, Phys. Rev. B **62**, 1171 (2000).

¹⁹E. E. Fullerton, J. S. Jiang, M. Grimsditch, C. H. Sowers, and S. D. Bader, Phys. Rev. B **58**, 12 193 (1998).

²⁰J. S. Jiang, G. P. Felcher, A. Inomata, R. Goyette, C. S. Nelson, and S. D. Bader, J. Vac. Sci. Technol. A **18**, 1264 (2000).

²¹P. A. Dowben, Y.-G. Kim, S. Baral-Tosh, G. O. Ramseyer, C. Hwang, and M. Onellion, J. Appl. Phys. **67**, 5658 (1990).

²²K. Perkins, C. Hwang, M. Onellion, Y.-G. Kim, and P. A. Dowben, Thin Solid Films **198**, 317 (1991).

²³D. C. Mancini, S. Varma, J. K. Simons, R. A. Rosenberg, and P. A. Dowben, J. Vac. Sci. Technol. B **8**, 1804 (1990).

²⁴D. Welipitiya, C. N. Borca, P. A. Dowben, I. Gobulokoglu, H. Jiang, B. W. Roberson, and J. Zhang, Mater. Res. Soc. Symp. Proc. **475**, 257 (1997).

²⁵C. N. Borca, D. Welipitiya, S. Adenwalla, and P. A. Dowben, Phys. Low-Dimens. Struct. **11**, 173 (1997).

²⁶C. B. Stagescu, X. Su, D. E. Eastman, K. N. Altmann, F. J. Himpsel, and A. Gupta, Phys. Rev. B **61**, R9233 (2000).

²⁷J. Noguez and I. K. Schuller, J. Magn. Magn. Mater. **192**, 203 (1999).

²⁸E. F. Kneller and R. Hawig, IEEE Trans. Magn. **27**, 3588 (1991).

²⁹Practical Surface Analysis: Auger and X-ray Photoelectron Spectroscopy, edited by D. Briggs and M. P. Seah (Wiley, New York, 1996), Vol. 1.

³⁰C. Arnone, M. Rothschild, J. G. Balck, and D. J. Erlich, Appl. Phys. Lett. **48**, 1018 (1986).

³¹H. Dulli, E. W. Plummer, P. A. Dowben, J. Choi, and S.-H. Liou, Appl. Phys. Lett. **77**, 88 (2000).

³²D. Ristoiu, J. P. Nozieres, C. N. Borca, B. Borca, and P. A. Dowben, Appl. Phys. Lett. **76**, 2349 (2000).